

DOI: 10.1002/((please add manuscript number))

Article type: Communication

**Self-Calibrating Mechanochromic Fluorescent Polymers Based on Encapsulated Excimer-Forming Dyes**

*Céline Calvino<sup>1</sup>, Anirvan Guha<sup>1</sup>, Christoph Weder<sup>1,\*</sup>, Stephen Schrettl<sup>1,\*</sup>*

C. Calvino, A. Guha, Prof. C. Weder, Dr. S. Schrettl  
Adolphe Merkle Institute, University of Fribourg  
Chemin des Verdiers 4, CH-1700, Fribourg, Switzerland  
E-mail: christoph.weder@unifr.ch, stephen.schrettl@unifr.ch

Keywords: aggregachromic, bioinspired, excimer formation, mechanochromic, microcapsules

**Abstract**

While mechanochemical transduction principles are omnipresent in nature, mimicking these in artificial materials is challenging. The ability to reliably detect the exposure of man-made objects to mechanical forces is, however, of great interest for many applications, including structural health monitoring and tamper-proof packaging. A useful concept to achieve mechanochromic responses in polymers is the integration of microcapsules, which rupture upon deformation and release a payload causing a visually detectable response. Herein, we report that this approach can be used to create mechanochromic fluorescent materials that show a direct and ratiometric response to mechanical deformation. This was achieved by filling poly(urea-formaldehyde) microcapsules with a solution of a photoluminescent aggregachromic cyano-substituted oligo(*p*-phenylene vinylene) and embedding these particles in poly(dimethylsiloxane). The application of mechanical force by way of impact, incision, or tensile deformation opens the microcapsules and releases the fluorophore in the damaged area. Due to excimer formation, the subsequent aggregation of the dye furnishes a detectable fluorescence color change. With the emission from unopened microcapsules as built-in reference, the approach affords materials that are self-calibrating. This new concept appears to be readily applicable to a range of polymer matrices and allows for the straightforward assessment of their structural integrity.

**Main Text**

A wide range of molecules, molecular assemblies, materials, and systems that respond to external stimuli in a selective and effective manner can be found in living systems,<sup>[1]</sup> where such components fulfill essential biological functions that sustain life. In addition to many other biological transduction schemes,<sup>[2,3]</sup> mechanochemical transduction processes, which couple mechanical and chemical events, are widespread in living organisms.<sup>[4-7]</sup> For example, a sense of touch is experienced when force is transduced to the cell membrane and the resulting tension leads to conformational changes of the mechanosensitive ion-channels,<sup>[8,9]</sup> and the bioluminescence of dinoflagellates occurs when shear forces deform the cell membranes.<sup>[10-12]</sup> Inspired by such principles, the idea to create artificial materials that display useful macroscopic responses in response to mechanically induced processes has gained significant traction,<sup>[13,14]</sup> although, with few exceptions,<sup>[15-17]</sup> vastly simplified designs are explored.<sup>[18-21]</sup> Mechanochromic polymers, which change their absorption and/or emission color upon (excessive) mechanical stress, are one subset of this growing class of responsive materials whose behavior is useful for a variety of applications, ranging from structural health monitoring to packaging that indicates tampering.<sup>[22-24]</sup>

A number of different concepts to impart polymers with mechanochromic behavior have been developed.<sup>[24-26]</sup> One prominent design approach involves the introduction of color-changing mechanophores into the macromolecules, *i.e.*, motifs that are designed to reversibly or irreversibly change their optical characteristics in response to mechanical stress. Prominent examples include the ring-opening of the colorless spiropyran moiety to a colored merocyanine,<sup>[27]</sup> the light-emission upon rupture of polymer networks with cross-links featuring a four-membered dioxetane ring,<sup>[28]</sup> and the mechanically induced homolytic cleavage of diarylbibenzofuranone that furnishes stable blue-colored radicals.<sup>[29]</sup> The use of excimer-forming aggregachromic dyes, which change their fluorescence properties upon

aggregation/dispersion, is another promising approach that affords polymers with mechanoresponsive luminescence.<sup>[30-34]</sup> The concept was first demonstrated by integrating a cyano-substituted oligo(*p*-phenylene vinylene) (cyano-OPV) into linear low-density polyethylene.<sup>[35,36]</sup> Even at dye concentrations below 1% w/w, phase separation of the molecules from the polymer yields nanoscale aggregates, which display red excimer emission. The mechanical deformation of such blends causes the breakup of these dye aggregates, concomitant with a change to green monomer emission. While the concept could be extended to other polymers including polyesters,<sup>[37]</sup> polyamides,<sup>[38]</sup> polyurethanes,<sup>[39]</sup> and fluoropolymers,<sup>[40]</sup> as well as dyes that, *e.g.*, change their absorption color,<sup>[41]</sup> achieving adequate stress transfer between a matrix polymer of interest and the chromophore aggregates is not always trivial.

Another useful concept to realize mechanochromic responses in polymers is the integration of microcapsules, which rupture upon deformation and release a payload that causes a visually detectable response,<sup>[25,42]</sup> for example on account of a chemical reaction between a (latent) chromophore and an auxiliary reagent or catalyst embedded in the polymeric matrix.<sup>[43]</sup> Recent examples of microcapsule-containing mechanochromic polymer composites include systems in which released thiols react with a polymer-dispersed rhodamine-based profluorophore to cause a fluorescence turn-on response,<sup>[44]</sup> 1,3,5,7-cyclooctatetraene released from microcapsules polymerizes upon release with a metathesis catalyst in the matrix and causes a color change,<sup>[45,46]</sup> pH-sensitive dyes released from microcapsules interact with residual free amines in the matrix to cause a color change,<sup>[47]</sup> hexamethylbenzene and chloranil released from microcapsules form a highly colored charge-transfer complex,<sup>[48]</sup> and an aggregation-induced emission luminogen released from microcapsules causes a fluorescence turn-on upon solvent evaporation and dye aggregation.<sup>[49]</sup>

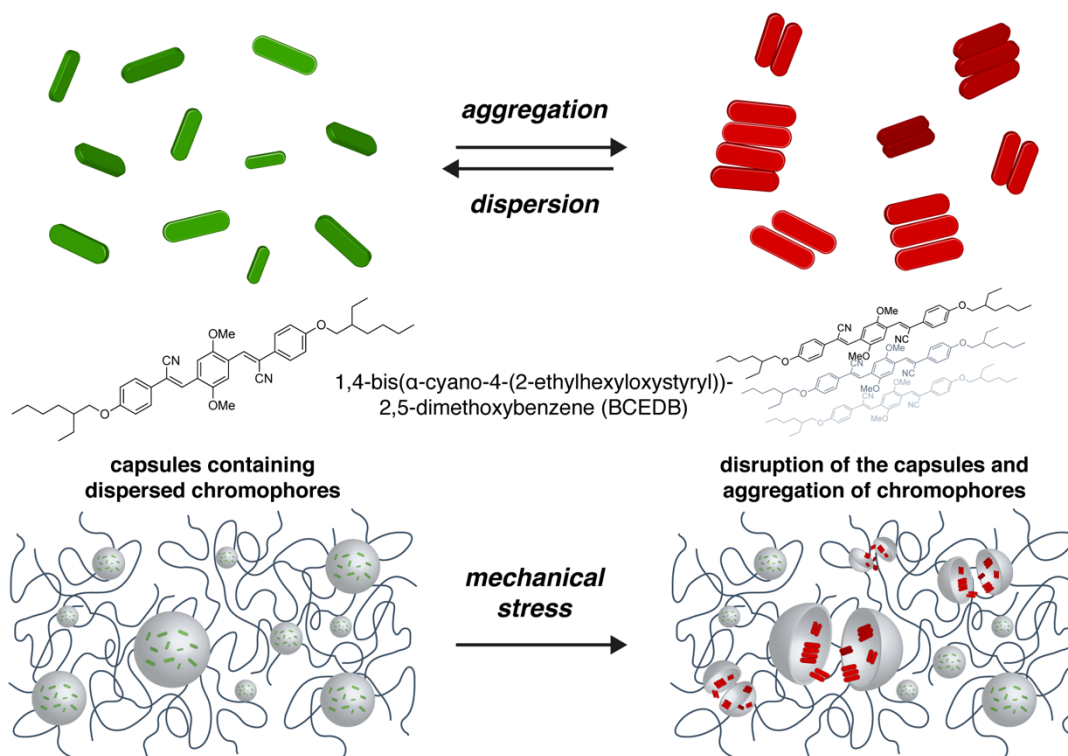


**Figure 1.** Schematic representation of the principles at play in self-calibrating mechanochromic fluorescent polymers based on encapsulated excimer-forming dyes. The framework combines the concepts of aggregation-induced excimer-formation of an aggregachromic fluorescent dye (such as the cyano-OPV derivative BCEDB) and the mechanically controlled release from microcapsules containing solutions of the latter.

We herein report a novel approach to mechanochromic fluorescent polymers that show a direct and ratiometric response to mechanical deformation. The framework combines the concepts of aggregation-induced excimer-formation of a fluorescent dye and the mechanically controlled release from microcapsules in which the latter is embedded. As a first embodiment of this idea, poly(urea-formaldehyde) microcapsules were filled with a hexyl acetate solution of an ethylhexyl-substituted cyano-OPV derivative and embedded in poly(dimethylsiloxane). Upon mechanical impact, incision, or tensile deformation, the microcapsules rupture and release the fluorescent dye into the damaged area. On account of excimer formation, the subsequent aggregation of the dye molecules leads to an easily detectable change of the

fluorescence color (**Figure 1**). The approach combines two attractive features. On the one hand, the mechanically induced response is a fluorescence color *change* (rather than a turn on or turn off effect) so that the response is always a ratiometric signal that renders the materials self-calibrating and makes quantitative assessment absolutely straightforward. On the other hand, this simple approach appears to be readily applicable to a broad range of polymer matrices and allows for the assessment of the structural integrity of composite materials featuring these capsules.

From the various aggregachromic dyes that have been previously reported,<sup>[22,24,30,31]</sup> we selected the excimer-forming fluorescent cyano-OPV derivative 1,4-bis( $\alpha$ -cyano-4-(2-ethylhexyloxystyryl))-2,5-dimethoxybenzene (BCEDB) for the present work.<sup>[50]</sup> The emission maxima of molecular solutions and solid-state samples of this dye differ considerably and the two peripheral ethylhexyloxy groups lead to a relatively high solubility in a range of organic solvents. For example, in hexyl acetate, a common industrial solvent and synthetic flavor ( $bp = 164\text{--}176\text{ }^{\circ}\text{C}$ ,  $P_{(20^{\circ}\text{C})} = 0.16\text{ kPa}$ ),<sup>[51,52]</sup> BCEDB can be dissolved at a concentration of up to  $11.6\text{ mg/mL}$  ( $c = 17\text{ mmol/L}$ ). A comparison of the fluorescence spectra of a dilute ( $c = 0.09\text{ }\mu\text{mol/L}$ ) hexyl acetate solution of BCEDB (which features maxima at 502 and 534 nm) and the microcrystalline solid obtained after drying a hexyl acetate solution (with maxima at 566 and 611 nm) showcases the significant bathochromic shift that occurs upon aggregation (**Figure 2a**). These spectral changes are accompanied by a readily detectable color change from bright green to orange (**Figure 2b**). Note that BCEDB, like other cyano-OPV derivatives,<sup>[53,54]</sup> can adopt different solid-state structures with dissimilar emission characteristics. For example when precipitated into methanol, BCEDB forms a red-light emitting powder with an emission maximum centered around 619 nm.<sup>[50]</sup>

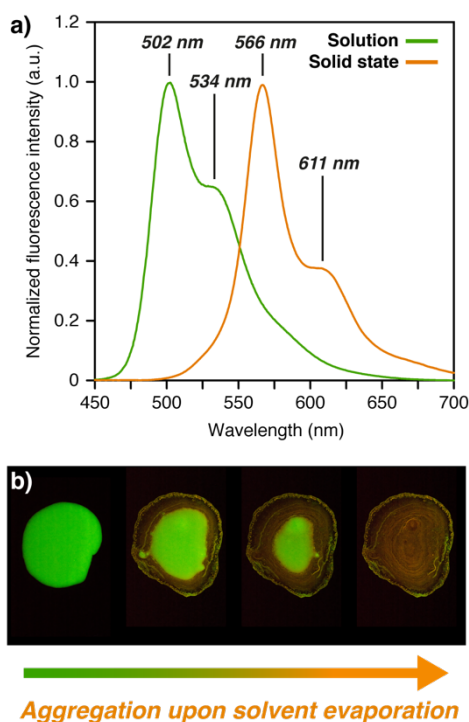


**Figure 2.** Emission properties of the excimer-forming chromophore used. **a)** Fluorescence spectra of 1,4-bis( $\alpha$ -cyano-4-(2-ethylhexyloxystyryl))-2,5-dimethoxybenzene (BCEDB) in hexyl acetate solution ( $c = 0.09 \mu\text{mol/L}$ ) and as a microcrystalline solid obtained by drying a hexyl acetate solution ( $c = 15 \text{ mmol/L}$ ) under ambient conditions in the fume hood. The spectra were recorded upon excitation at 438 nm. **b)** Pictures showing the fluorescence color change upon drying of a drop of a solution of BCEDB in hexyl acetate ( $c = 15 \text{ mmol/L}$ ). The images were taken under illumination with 365 nm UV light.

Based on these initial findings, we pursued the preparation of poly(urea formaldehyde) (PUF) microcapsules filled with a hexyl acetate solution of BCEDB. Such microcapsules (which hereafter are referred to as “BCEDB microcapsules”) were obtained by an oil-in-water emulsion polycondensation of urea, resorcinol, formaldehyde, and poly(ethylene-*alt*-maleic anhydride) that was carried out at 55 °C in the presence of 1-octanol and a solution of BCEDB in hexyl acetate ( $c = 5.4 \text{ mmol/L}$ ).<sup>[48,55]</sup> A portion of the BCEDB microcapsules thus made was mechanically crushed, thoroughly washed with chloroform, and the solid fragments were isolated and dried under high vacuum. Based on the weight of the solid residue, a weight fraction of 95% w/w was determined for the BCEDB/hexyl acetate cargo. Thermogravimetric

measurements reveal good thermal stability of the capsules, with a weight loss of 5% and 22 upon dynamic heating to 130 °C and 220°C, respectively, due to the evaporation of hexyl acetate (**Figure S1** in the Supporting Information). The analysis of optical microscopy and scanning electron microscopy (SEM) images reveals that the BCEDB microcapsules are spherical with an average size of  $67 \pm 22 \mu\text{m}$  and a shell thickness of  $15 \pm 8 \mu\text{m}$  (**Figure S2–S4** in the Supporting Information).

Under illumination with UV light ( $\lambda = 365 \text{ nm}$ ), the BCEDB microcapsules displayed the characteristic intense green, monomer-dominated emission of the molecularly dispersed BCEDB chromophores (**Figure 3a,b**). The fluorescence spectrum (**Figure 3f**) is virtually identical with the one obtained for the BCEDB solution (**Figure 2a**). Moreover, the same green fluorescence was observed under the optical microscope when the sample was illuminated by UV light ( $\lambda = 365 \text{ nm}$ ), whereas application of a red filter that limits emission to 580–630 nm resulted in a complete loss of fluorescence, indicating the absence of excimers in the as-prepared capsules (see **Figure S3** in the Supporting Information). When the BCEDB microcapsules were broken, the evaporation of the solvent eventually led to the aggregation of the BCEDB as indicated by the concomitant appearance of the characteristic orange fluorescence color (**Figure 3c,d**) and the appearance of additional, red-shifted bands in the fluorescence spectra (**Figure 3f**). Similarly, locally damaging a fraction of the BCEDB microcapsules by incision with a razor-blade led to a localized change of the fluorescence emission from green to orange in the damaged regions (**Figure 3e**). A sequence of emission spectra acquired at different times after rupturing the capsules reveals that the optical properties first remain virtually unchanged and monomer-dominated emission is observed for a period of time (under the experimental conditions applied for about 20 min), after which a rapid transition to excimer-rich emission is observed, arguably because the solvent has evaporated (**Figure 3f**).



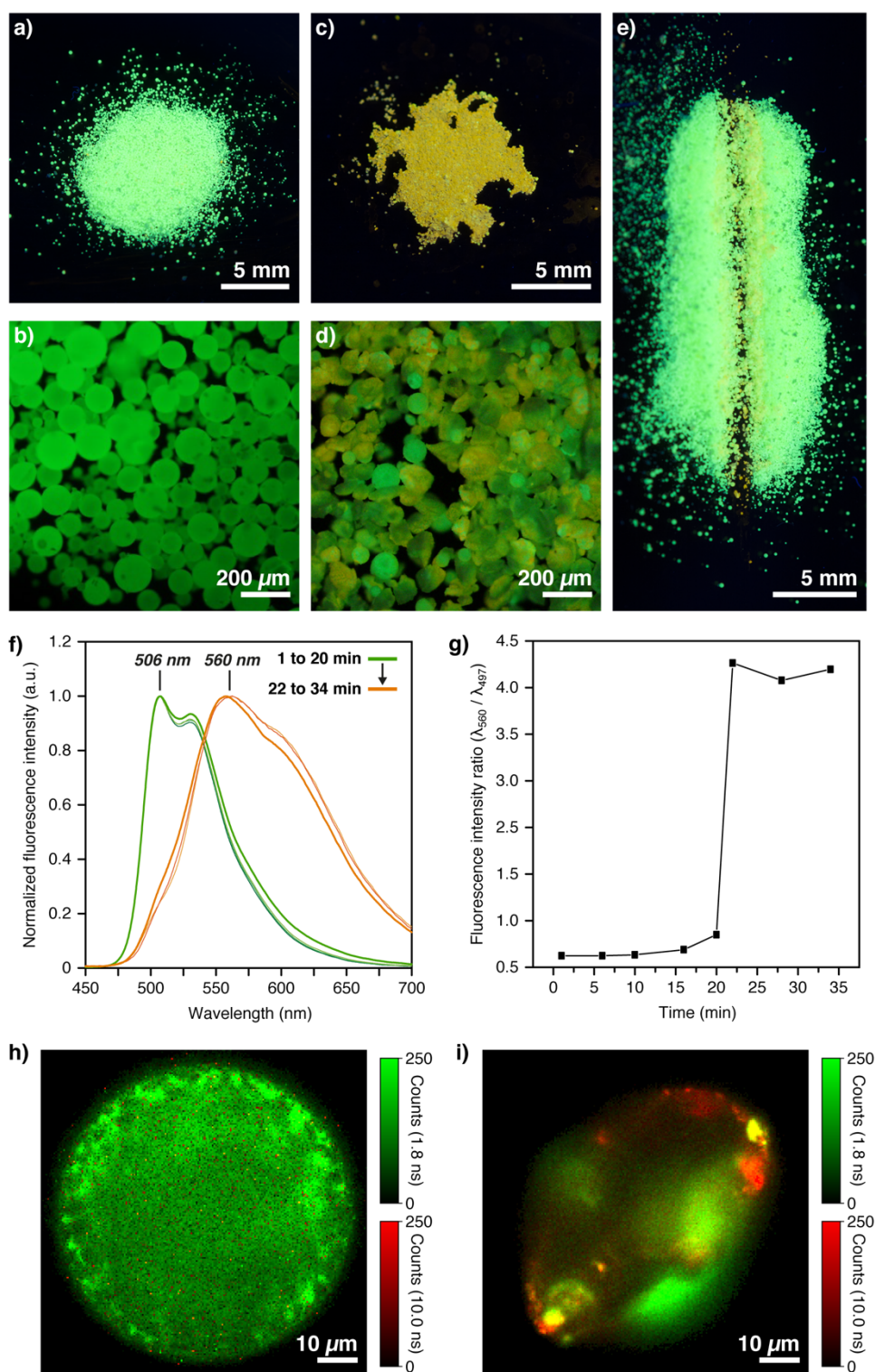


**Figure 3.** Fluorescent poly(urea formaldehyde) microcapsules filled with a hexyl acetate solution of BCEDB. **a,c)** Photographs and **b,d)** optical micrographs of such BCEDB microcapsules before (**a,b**) and 30 min after (**c,d**) breaking them by compression between two glass slides and removing one of the slides to allow for solvent evaporation. **e)** Photograph taken 30 min after incision of the microcapsules with a razor blade. **f)** Fluorescence spectra of the BCEDB microcapsules 1–34 min after breaking them as in (**c,d**). **g)** Plot of the ratio of the

excimer to monomer emission intensities ( $I_E/I_M$ ) recorded at 560 and 497 nm extracted from the data shown in (f). The images shown in a-e were recorded under illumination with 365 nm UV light. (h) Fluorescence lifetime imaging microscopy (FLIM) of a single intact microcapsule almost exclusively shows monomer emission with a lifetime of 1.8 ns (green intensity). (i) FLIM micrograph of a crushed capsule showing substantial excimer emission with a lifetime of 10.0 ns (red intensity).

This behavior is clearly reflected in the ratio of the excimer to monomer emission intensities ( $I_E/I_M$ ) recorded at 560 nm (excimer emission maximum) and at 497 nm (**Figure 3g**). The latter wavelength was chosen instead of the monomer emission maximum (506 nm), in order to minimize any contribution from excimer emission. Plots of  $I_E/I_M$  serve as a first indication for the self-calibrating feature as changes in the acquisition parameters for the spectroscopy measurements (*e.g.* the distance between the tip of the optical fiber used and the sample, the acquisition time, or the incidence angle) with the same batch of the BCEDB microcapsules showed that the fluorescence intensity ratio remained constant (**Figure S5a** in the Supporting Information). Moreover, without inflicting mechanical damage, no changes of the fluorescence color or the emission spectra were observed over the course of weeks when the BCEDB microcapsules were stored under ambient conditions. Microcapsules containing only hexyl acetate in the core did not fluoresce before or after being ruptured (**Figure S6** in the Supporting Information) and it appears conceptually straightforward to exchange the hexyl acetate against solvents with higher or lower evaporation rates in order to obtain systems with different aggregation kinetics. In this context, the cyano-OPV loaded capsules, may be of interest in their own right, for example, as a means to conduct single capsule experiments and monitor their structural integrity, or as micrometer-sized markers with an integrated fluorescence response. Fluorescence lifetime imaging microscopy offers the possibility to investigate the effects of mechanical damage at the scale of single capsules (**Figure 3h,i** and **Figure S7** in the Supporting Information). Thus, lifetime images of the intact capsules

primarily exhibit monomer emission with a lifetime of 1.8 ns, whereas micrographs taken 30 min after capsules were crushed show various regions of excimer emission with a longer lifetime of 10.0 ns.

To investigate the usefulness of the BCEDB microcapsules to create self-calibrating mechanochromic fluorescent polymer systems, they were first incorporated in poly(dimethylsiloxane) (PDMS), which was selected as a testbed on account of its high transparency and extensibility, as well as the fact that previous studies revealed efficient stress transfer to microcapsules embedded in this matrix.<sup>[56,57]</sup> Thus, samples were prepared by mixing a silicone base with 10% w/w of the curing agent (Sylgard<sup>®</sup> 184) and 10% w/w of the BCEDB microcapsules. After careful stirring (to ensure a good dispersion and to retain the structural integrity of the capsules) the mixture was transferred into an aluminum or poly(tetrafluoroethylene) (PTFE) mold and cured for 40 min at 80 °C. This process was used to produce cylindrical disks with diameters of 28 - 70 mm and thicknesses of 6 - 40 mm, as well as dog-bone-shaped films with a length of 75 mm and a cross-section of 4 × 7 mm. Under illumination with UV light ( $\lambda = 365$  nm) the resulting composites displayed the characteristic intense green fluorescence (**Figure 4a** and **Figure S6** in the Supporting Information) of the neat BCEDB microcapsules (**Figure 3a,b**) and the fluorescence spectra display exclusively monomer emission (**Figure 4c**), even when stored in ambient conditions for weeks (**Figure S5b** in the Supporting Information). These findings confirm that the thermal treatment during curing did not lead to aggregation of the chromophores or loss of the efficient encapsulation. A comparison with the emission spectra of the neat PDMS matrix and a reference composite featuring capsules solely filled with hexyl acetate confirmed that the fluorescence exclusively originates from the dispersed BCEDB chromophores (**Figure S6** in the Supplementary Information) and optical microscopy images corroborate that the capsules were well-dispersed within the PDMS matrix (**Figure S6** in the Supplementary Information).

With these data in hand, we explored the mechanochromic response of the BCEDB microcapsule containing PDMS composites upon mechanical stress in the form of incision, compressive stress, tensile deformation, or impact. Thus, local damage was first inflicted by cutting through the composite with a knife, which led to a change of the fluorescence to the orange excimer emission color as evidenced by photographs and fluorescence micrographs of the damaged region taken after 30 min (**Figure 4a,b**), which was chosen for all experiments as the delay between application of mechanical stress and sample inspection to allow for excimer formation to complete under ambient conditions. While the localized change of the fluorescence color to orange was clearly observed along the entire cross-section of the cut, such minor damages are challenging to discern spectroscopically due to the diffuse nature of the emission and the experimental limitations of facile measurements in reflection geometry with fiber optics, notably the acquisition spot size of ca. 800  $\mu\text{m}$ . Thus, the emission spectra recorded in the damaged region display only minor changes, as the surrounding intact microcapsules furnished a strong background signal (**Figure 4c**).

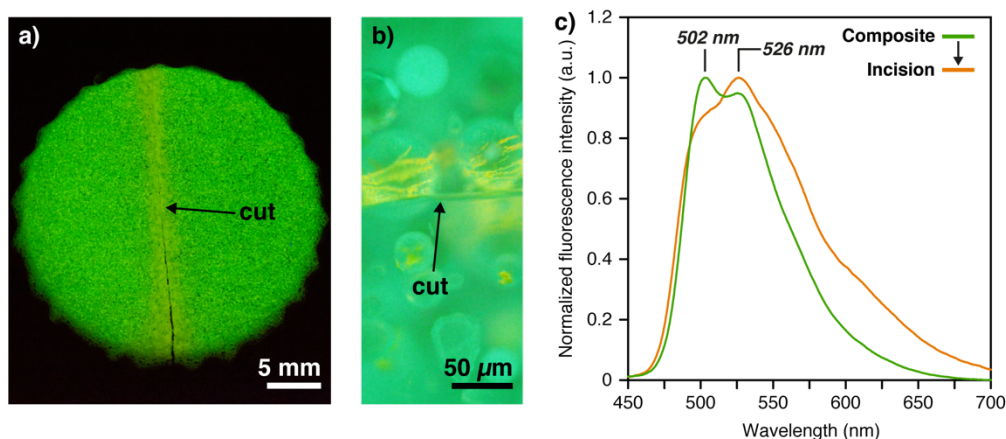


**Figure 4.** Mechanochromic composites of polydimethylsiloxane (PDMS) and poly(urea formaldehyde) microcapsules filled with hexyl acetate and BCEDB. **a)** Picture of a PDMS film containing 10% w/w of BCEDB microcapsules after incision with a knife, displaying a fluorescence color change from green to orange along the cut. **b)** Fluorescence microscopy image of the damaged area shown in (a). **c)** Comparison of the fluorescence spectra of the

PDMS/microcapsule composite before and after incision with a knife ( $\lambda_{\text{ex}} = 365 \text{ nm}$ ). The images shown in **a-b** were recorded under illumination with 365 nm UV light.

In order to trigger a mechanochemical response in a sufficiently large area to conduct spectroscopic experiments, the BCEDB microcapsule containing PDMS composites were subjected to impact tests, which involved a conical missile (51 g) that was dropped through a tube from distances between 1 and 44 cm (**Figure S8** in the Supplementary Information). At distances of greater than 5 cm, the impact of the missile immediately (<1 min) induced a change of the fluorescence color from green to orange (**Figure S9** in the Supplementary Information). The response was much faster than when the neat BCEDB microcapsules were damaged (*vide supra*), suggesting that the solvent rapidly diffuses through the PDMS matrix, causing an immediate aggregation of the cyano-OPV chromophores. The mechanochromic response can be visually detected or discerned from the fluorescence spectra (measured after 30 min, **Figure S9** in the Supplementary Information), but the relation of impact and optical changes is best seen from plots of the ratio of  $I_E/I_M$  recorded at 560 and 497 nm against the impact distance (**Figure 5a,b**). Intriguingly, for impact distances between 0 to 5 cm (corresponding to kinetic energies of up to 1 J), the evaluation of data from three separate samples showed that  $I_E/I_M$  linearly scales with the distance (**Figure 5a,b**). No further changes are observed at higher impact distances, presumably because of a limit of the stress transfer from the matrix to the capsules, the high diameter dependence of the failure of poly(urea-formaldehyde) capsules,<sup>[58]</sup> and the potential crack deflection from the capsules.<sup>[46]</sup>

We reiterate that this analysis is enabled by the fact that intact capsules filled with molecularly dispersed BCEDB constitute an internal standard that can be employed to express the extent of aggregate formation and thereby indirectly the degree of damage to the material and reproducible results are furnished across samples. Moreover, the same measurements

were repeated after three weeks and the fluorescence intensity ratio as a ratiometric signal was found to remain constant (**Figure S5b** in the Supplementary Information).

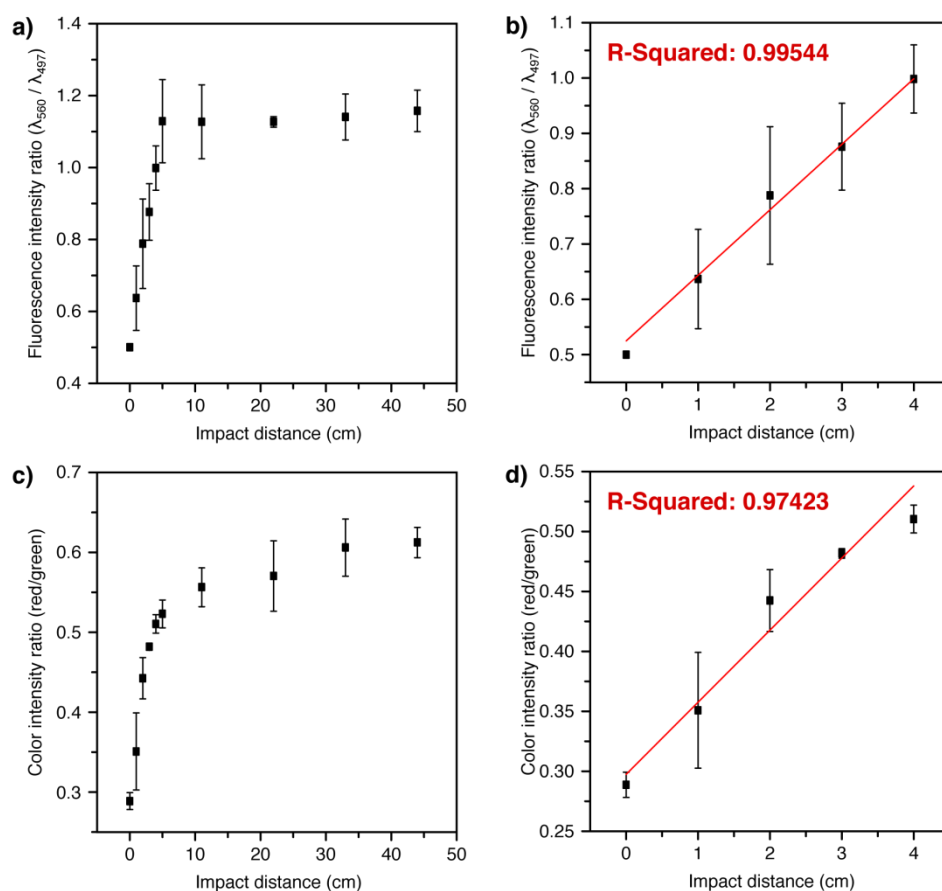


**Figure 5.** Analysis of the mechanochromic response of BCEDB microcapsule containing PDMS films upon impact of a missile. **a)** Plot of the ratio of the excimer to monomer emission intensities ( $I_E/I_M$ ) recorded at 560 and 497 nm as a function of impact distance (evaluation of three samples). **b)** Magnification of the low-impact distance range shown in (a) and a linear fit to the data. **c)** Plot of the intensity ratio in the red and green color channels ( $I_R/I_G$ ) obtained by color analysis of pictures recorded under illumination with UV light ( $\lambda = 365$  nm, evaluation of pictures of three samples). **d)** Magnification of the low-impact distance range shown in (c) and a linear fit to the data.

In addition to the spectroscopic evaluation of the damaged regions of the specimen by means of fluorescence spectroscopy, pictures of these samples that were recorded under illumination with UV light ( $\lambda = 365$  nm) were subjected to a RGB color analysis (see Supplementary



Information for details) and the intensities in the green and red color channels were employed as proxies for monomer and excimer emission, respectively. Gratifyingly, the plots of the intensity ratio thus obtained versus the impact distance (**Figure 5c,d**) mirror the corresponding graphs based on the spectroscopic emission intensity ratios ( $I_E/I_M$ ). Thus, the data show strikingly that the fluorescence color analysis of images recorded under UV illumination can be used as a facile (automated) means to quantify the mechanochromic response of BCEDB microcapsule containing PDMS composites.

In addition to the above-discussed impact experiments, the mechanochromic response of BCEDB microcapsule containing PDMS films to uniaxial deformation was investigated. For this purpose, the material was cured in dog-bone-shaped PTFE molds (length 75 mm, cross-section  $4 \times 7$  mm). The application of tensile stress to similar composites has been previously investigated, and deformation beyond a strain of 1.5% was found to lead to failure of PUF microcapsules and release of the cargo.<sup>[48,57]</sup> In the context of the present investigation, the BCEDB microcapsule containing PDMS were stretched until failure, which typically occurred at engineering strains above 60% (**Figure S10** in the Supplementary Information). Tensile deformation of the samples accordingly damaged a significant fraction of the microcapsules and a strong visual fluorescence change from green to orange across the sample was observed (**Figure 6a**). Capsules in the clamped portions of the samples were also damaged resulting in orange excimer emission, while this was not observed in the low-stress regions. The corresponding fluorescence spectra display the two characteristic bands around 560 and 608 nm corresponding to aggregated BCEDB chromophores, and the relative intensity of these bands is most prominent in the failed sample region that experienced the highest tensile load (**Figure S10** in the Supplementary Information). Spectra were also acquired at various distances between the failed segment of the sample and the intact sample region, which allowed plotting  $I_E/I_M$  as a function of position along the sample (**Figure 6b**). In accordance with the

distribution of stress in the dog-bone-shaped sample, an increasing  $I_E/I_M$  ratio is observed in close proximity to the failed region. Similar results were obtained when a color analysis of pictures recorded under illumination with UV light ( $\lambda = 365$  nm) was carried out and the intensity ratio in the green and red color channels was compared (**Figure 6c**). In this case, however, the traces of the color analysis and fluorescence intensities ( $I_E/I_M$ ) did not mirror each other exactly, presumably because the large acquisition spot size (ca. 800  $\mu\text{m}$ ) limits the spatial resolution of the spectroscopic analysis, whereas the picture analysis offers a much higher resolution (see Supplementary Information for details).

In order to investigate the effect of compressive stresses, cylindrically shaped samples of the BCEDB microcapsule containing PDMS composite with diameters of 28 mm and a thickness of 6 mm were prepared in cylindrical aluminum molds (**Figure S11** in the Supplementary Information). When these samples were manually compressed, the microcapsules were damaged as evidenced by the observed change of the fluorescence color to orange. The change became more pronounced over the course of 30 min and a comparison of the corresponding fluorescence spectra before and after the compression clearly shows the appearance of the bands at 560 and 608 nm associated with excimer formation (**Figure S12** in the Supplementary Information). In compressive stress-strain measurements, the cylindrical specimen structurally failed above compressive strains of 60% (**Figure S12** in the Supplementary Information).



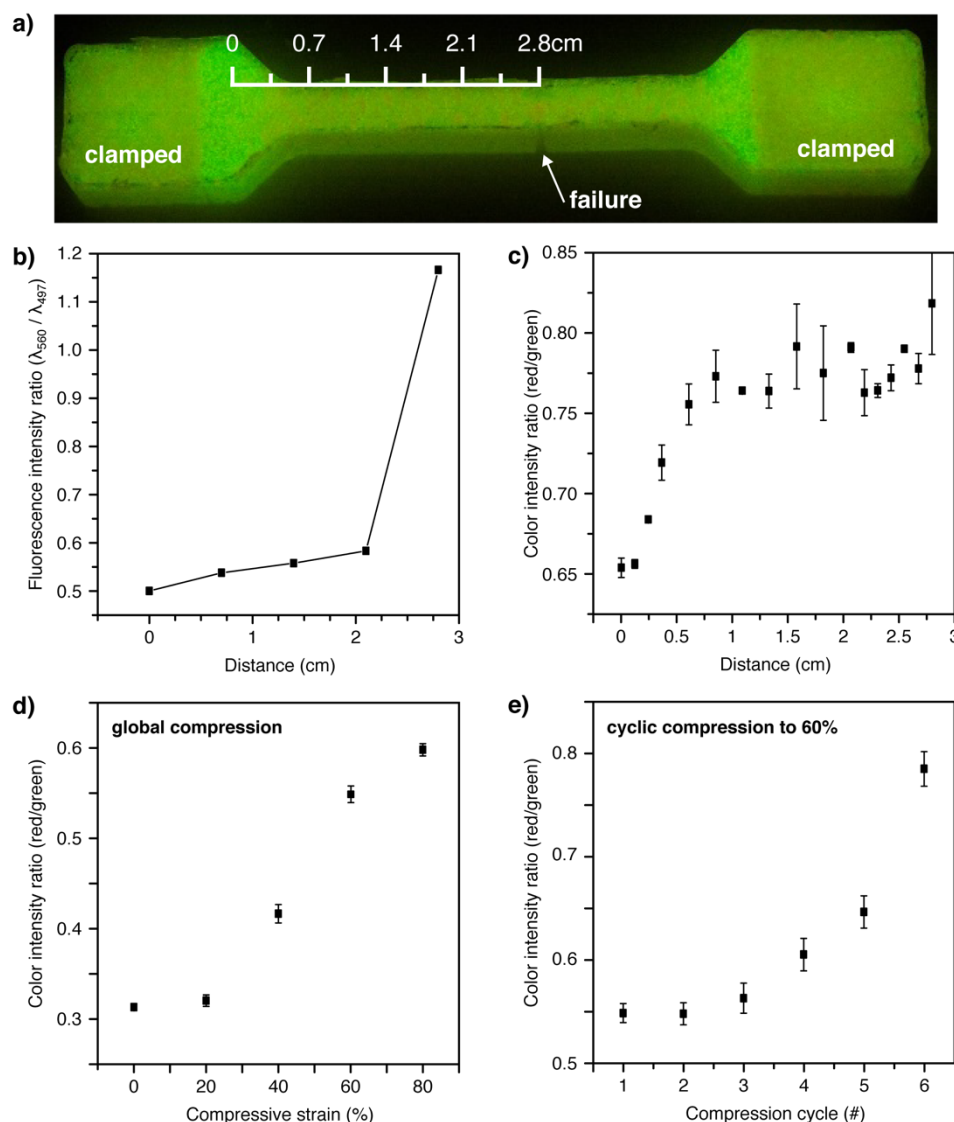


**Figure 6.** Analysis of the mechanochromic response of BCEDB microcapsule containing PDMS films upon tensile deformation and compression. **a)** Picture of a PDMS film containing 10% w/w of BCEDB microcapsules after tensile deformation, displaying a fluorescence color change from green to orange across the sample in the narrow section and the clamped portions. **b)** Plot of the ratio of the excimer to monomer emission intensities ( $I_E/I_M$ ) recorded at 560 and 497 nm as a function of distance to the failed sample region. **c)** Plot of the intensity ratio in the red and green color channels ( $I_R/I_G$ ) obtained by color analysis of pictures recorded under illumination with UV light ( $\lambda = 365$  nm) as a function of distance to the failed sample region (evaluation of three profiles). **d)** Plot of  $I_R/I_G$  as a function of compressive strain obtained by color analysis of pictures of compressed samples. **e)** Plot of  $I_R/I_G$  as a function of the number of compressions to a strain of 60% obtained by color analysis of the corresponding pictures (evaluation of three sample regions). The analyzed images were recorded under illumination with 365 nm UV light.

To investigate the visually and spectroscopically discernible fluorescence changes, compressive strains between 20 and 80% were applied and kept up for 2 min to reach compression stability throughout the sample. As seen in photographs taken under UV light illumination ( $\lambda = 365$  nm) after release of the strain, the samples exhibit an appreciable fluorescence change above strains of 40% (**Figure S11** in the Supplementary Information), as also confirmed by the fluorescence spectra that show an increase of the excimer signal intensities at 560 and 608 nm with a simultaneous decrease of the monomer emission intensity (**Figure S12** in the Supplementary Information). The spectra suggest that a significant part of the fluorescence originates from BCEDB chromophores that remain dispersed inside intact capsules and recorded microscopy images indeed showed that a fraction of the capsules remained intact, even at compressive strains of up to 80% at which failure of the PDMS matrix was observed. The stress transfer from a single compression cycle therefore appears to only damage a fraction of the embedded capsules. Indeed, when multiple compression cycles to a strain of 60% were performed, a step-wise increase of the excimer emission was observed in the corresponding spectra (**Figure S12** in the Supplementary Information). The analysis of the mechanical damage by means of a comparison of the fluorescence intensity of the monomer and excimer emission ( $I_E/I_M$ ) turned out to be challenging in the case of the compression experiments. Thus, the application of mechanical stress across the large sample in these compressive stress-strain experiments leads to a broad and uneven distribution of damaged microcapsules and recorded fluorescence spectra only locally capture the monomer/excimer ratio. By contrast, representative results were readily obtained by color analysis of pictures of the corresponding specimen that were recorded under illumination with UV light ( $\lambda = 365$  nm) and a comparison of the intensity ratio in the green and red color channels. The plot of the red-to-green intensity ratio ( $I_G/I_R$ ) after global compression to different strains between 0 and 80% readily furnished a direct correlation

between the applied mechanical stress and the color intensity based on the increased orange excimer to green monomer concentration across the specimen (**Figure 6d**). Moreover, a corresponding ratiometric response was also obtained for cyclic compression experiments in which the sample was repeatedly compressed to the same strain (60%) and a color analysis was performed with pictures taken after each cycle (**Figure 6e**).

In order to demonstrate that the design approach pursued here is *a priori* generally useful, the BCEDB microcapsules were also incorporated into an epoxy resin and a styrene-butadiene rubber (SBR). Thus, epoxy samples were prepared by mixing a commercial two-component epoxy resin and hardener (Araldite<sup>®</sup> crystal) with 10% w/w of the BCEDB microcapsules in an aluminum mold and, after careful stirring to ensure a good dispersion and retain the structural integrity of the capsules, the mixture was cured for 15 min at ambient temperature. Similarly, samples with an SBR matrix were prepared by swelling commercial SBR rubber in chloroform, addition of 10% w/w of the BCEDB microcapsules, careful stirring of the mixture, and solvent casting into an aluminum mold, followed by removal of residual solvent by drying under high vacuum. These processes produced cylindrically-shaped epoxy and SBR composites with diameters of 28 mm and a thickness of 6 mm. The samples displayed the characteristic intense green monomer fluorescence of the neat BCEDB microcapsules under illumination with UV light ( $\lambda = 365$  nm) (**Figure S13,S14** in the Supplementary Information). When these samples were damaged by incision with a razor blade, changes of the fluorescence color were also observed for these composites (**Figure S13,S14** in the Supplementary Information), indicating that the underlying principles can be readily transferred to other types of polymers, as long as the respective matrices allow for efficient solvent diffusion without concomitant dispersion of the chromophores.

To conclude, a versatile method to create new mechanoresponsive materials that show a ratiometric response to mechanical deformation was developed. The approach marries the

concepts of aggregation-induced excimer-formation of fluorescent dyes and the mechanically controlled release from microcapsules in which the latter are embedded. We show that such microcapsules can readily be prepared, that after encapsulation the dye molecules remain molecularly dissolved for months, and that rapid dye aggregation occurs upon breaking the capsules and evaporation of the solvent, concomitant with a pronounced fluorescence color change. The prepared microcapsules were integrated in silicone matrices and mechanical deformation of the composites in the form of impact, incision, or tensile deformation disrupted the capsules resulting in a release of the fluorescent solution into the damaged area, subsequent formation of excimers, and a concomitant, clearly visible change of the fluorescence color. In contrast to related approaches to mechanochromic polymers, the herein reported system that changes its fluorescence color so that the response is always a ratiometric signal that makes quantitative assessment straightforward. In addition to a spectroscopic evaluation of damaged sample regions, RGB color analyses of pictures of the fluorescent materials taken under UV light were found to constitute a facile means to quantify the mechanochromic response of the BCEDB microcapsule composites. This simple approach toward damage-sensing materials appears to be readily applicable to a range of polymer matrices and allows for the straightforward assessment of the structural integrity of composite materials.

## Supporting Information

Supporting Information is available from the Wiley Online Library: Supplementary Figures S1–S16 and a comprehensive account of all experimental details, including synthetic procedures, analytical data, and NMR spectra of all compounds.

## Acknowledgements

The authors thank S. Buchmann, M. Amrein, and C. Kress for help with some of the initial experiments. D. Moatsou, O. Rifaie-Graham, B. Wilts, and T. Moore are gratefully acknowledged for helpful discussions and comments on the manuscript. C.C., S.S., and C.W. gratefully acknowledge financial support through the National Center of Competence in Research (NCCR) Bio-Inspired Materials, a research instrument of the Swiss National Science Foundation (SNF), the Adolphe Merkle Foundation, and the European Research Council under the European Union's Seventh Framework Programme (FP7/2007-2013) / ERC grant agreement n° ERC-2011-AdG 291490-MERESPO.

Received: ((will be filled in by the editorial staff))

Revised: ((will be filled in by the editorial staff))

Published online: ((will be filled in by the editorial staff))

## References

- [1] C. de Duve, *Chem. Biodivers.* **2007**, *4*, 574.
- [2] W. Kolch, M. Halasz, M. Granovskaya, B. N. Kholodenko, *Nat. Rev. Cancer* **2015**, *15*, 515.
- [3] J. A. Papin, T. Hunter, B. O. Palsson, S. Subramaniam, *Nature Rev. Mol. Cell. Biol.* **2005**, *6*, 99.
- [4] A. Heinrichs, *Nature Rev. Mol. Cell. Biol.* **2009**, *10*, 163.
- [5] M. Chalfie, *Nature Rev. Mol. Cell. Biol.* **2009**, *10*, 44.
- [6] M. A. Wozniak, C. S. Chen, *Nature Rev. Mol. Cell. Biol.* **2009**, *10*, 34.
- [7] V. Vogel, M. Sheetz, *Nature Rev. Mol. Cell. Biol.* **2006**, *7*, 265.
- [8] L. Bianchi, *Mol Neurobiol* **2007**, *36*, 254.
- [9] Y. Tang, G. Cao, X. Chen, J. Yoo, A. Yethiraj, Q. Cui, *Biophys. J.* **2006**, *91*, 1248.
- [10] P. von Dassow, M. I. Latz, *J. Exp. Biol.* **2002**, *205*, 2971.
- [11] A. K. Chen, M. I. Latz, P. Sobolewski, J. A. Frangos, *Am J Physiol Regul Integr Comp Physiol* **2007**, *292*, R2020.
- [12] M. S, H. M, P. V. Dassow, L. M, F. J, *Journal of Comparative Physiology A: Sensory, Neural, and Behavioral Physiology* **2002**, *188*, 409.
- [13] N. Zhao, Z. Wang, C. Cai, H. Shen, F. Liang, D. Wang, C. Wang, T. Zhu, J. Guo, Y. Wang, X. Liu, C. Duan, H. Wang, Y. Mao, X. Jia, H. Dong, X. Zhang, J. Xu, *Adv. Mater.* **2014**, *26*, 6994.

- [14] C. Zhang, D. A. Mcadams, J. C. Grunlan, *Adv. Mater.* **2016**, 28, 6292.
- [15] N. Bruns, K. Pustelny, L. M. Bergeron, T. A. Whitehead, D. S. Clark, *Angew. Chem. Int. Ed.* **2009**, 48, 5666.
- [16] J. N. Brantley, C. B. Bailey, J. R. Cannon, K. A. Clark, D. A. Vanden Bout, J. S. Brodbelt, A. T. Keatinge-Clay, C. W. Bielawski, *Angew. Chem. Int. Ed.* **2014**, 53, 5088.
- [17] J. N. Brantley, C. B. Bailey, K. M. Wiggins, A. T. Keatinge-Clay, C. W. Bielawski, *Polym. Chem.* **2013**, 4, 3916.
- [18] C. Weder, *Nature* **2009**, 459, 45.
- [19] M. M. Caruso, D. A. Davis, Q. Shen, S. A. Odom, N. R. Sottos, S. R. White, J. S. Moore, *Chem. Rev.* **2009**, 109, 5755.
- [20] M. K. Beyer, H. Clausen-Schaumann, *Chem. Rev.* **2005**, 105, 2921.
- [21] A. L. Black, J. M. Lenhardt, S. L. Craig, *J. Mater. Chem.* **2011**, 21, 1655.
- [22] C. Weder, in *Encyclopedia of Polymeric Nanomaterials*, Springer Berlin Heidelberg, Berlin, Heidelberg, **2014**, pp. 1–11.
- [23] J. Li, C. Nagamani, J. S. Moore, *Acc. Chem. Res.* **2015**, 48, 2181.
- [24] C. Calvino, L. Neumann, C. Weder, S. Schrettl, *J. Polym. Sci. Part A: Polym. Chem.* **2017**, 55, 640.
- [25] J. F. Patrick, M. J. Robb, N. R. Sottos, J. S. Moore, S. R. White, *Nature* **2016**, 540, 363.
- [26] R. J. Wojtecki, M. A. Meador, S. J. Rowan, *Nature Mater.* **2011**, 10, 14.
- [27] D. A. Davis, A. Hamilton, J. Yang, L. D. Cremer, D. Van Gough, S. L. Potisek, M. T. Ong, P. V. Braun, T. J. Martinez, S. R. White, J. S. Moore, N. R. Sottos, *Nature* **2009**, 459, 68.
- [28] Y. Chen, A. J. H. Spiering, S. Karthikeyan, G. W. M. Peters, E. W. Meijer, R. P. Sijbesma, *Nature Chem.* **2012**, 4, 559.
- [29] K. Imato, T. Kanehara, T. Ohishi, M. Nishihara, H. Yajima, M. Ito, A. Takahara, H. Otsuka, *ACS Macro Lett.* **2015**, 4, 1307.
- [30] Y. Sagara, S. Yamane, M. Mitani, C. Weder, T. Kato, *Adv. Mater.* **2016**, 28, 1073.
- [31] Y. Sagara, T. Kato, *Nature Chem.* **2009**, 1, 605.
- [32] A. Pucci, G. Ruggeri, *J. Mater. Chem.* **2011**, 21, 8282.
- [33] F. Ciardelli, G. Ruggeri, A. Pucci, *Chem. Soc. Rev.* **2013**, 42, 857.
- [34] A. Pucci, M. Bertoldo, S. Bronco, *Macromol. Rapid Commun.* **2005**, 26, 1043.
- [35] C. Lowe, C. Weder, *Adv. Mater.* **2002**, 14, 1625.
- [36] B. R. Crenshaw, M. Burnworth, D. Khariwala, A. Hiltner, P. T. Mather, R. Simha, C. Weder, *Macromolecules* **2007**, 40, 2400.
- [37] M. Kinami, B. R. Crenshaw, C. Weder, *Chem. Mater.* **2006**, 18, 946.
- [38] A. Lavrenova, A. Holtz, Y. C. Simon, C. Weder, *Macromol. Mater. Eng.* **2016**, 301, 549.
- [39] B. R. Crenshaw, C. Weder, *Macromolecules* **2006**, 39, 9581.

- [40] J. Lott, C. Weder, *Macromol. Chem. Phys.* **2010**, *211*, 28.
- [41] J. Kunzelman, B. R. Crenshaw, M. Kinami, C. Weder, *Macromol. Rapid Commun.* **2006**, *27*, 1981.
- [42] A. P. Esser-Kahn, S. A. Odom, N. R. Sottos, S. R. White, J. S. Moore, *Macromolecules* **2011**, *44*, 5539.
- [43] M. A. White, *J. Chem. Educ.* **1998**, *75*, 1119.
- [44] E. T. A. van den Dungen, B. Loos, B. Klumperman, *Macromol. Rapid Commun.* **2010**, *31*, 625.
- [45] S. A. Odom, A. C. Jackson, A. M. Prokup, S. Chayanupatkul, N. R. Sottos, S. R. White, J. S. Moore, *ACS Appl. Mater. Interfaces* **2011**, *3*, 4547.
- [46] S. R. White, N. R. Sottos, P. H. Geubelle, J. S. Moore, M. R. Kessler, S. R. Sriram, E. N. Brown, S. Viswanathan, *Nature* **2001**, *409*, 794.
- [47] W. Li, C. C. Matthews, K. Yang, M. T. Odarczenko, S. R. White, N. R. Sottos, *Adv. Mater.* **2016**, *28*, 2189.
- [48] A. Lavrenova, J. Farkas, C. Weder, Y. C. Simon, *ACS Appl. Mater. Interfaces* **2015**, *7*, 21828.
- [49] M. J. Robb, W. Li, R. C. R. Gergely, C. C. Matthews, S. R. White, N. R. Sottos, J. S. Moore, *ACS Cent. Sci.* **2016**, *2*, 598.
- [50] B. R. Crenshaw, C. Weder, *Chem. Mater.* **2003**, *15*, 4717.
- [51] K.-G. Fahlbusch, F.-J. Hammerschmidt, J. Panten, W. Pickenhagen, D. Schatkowski, K. Bauer, D. Garbe, H. Surburg, in *Ullmann's Encyclopedia of Industrial Chemistry*, Wiley-VCH, Weinheim, Germany, **2003**, pp. 1–36.
- [52] D. Stoye, *Solvents*, Wiley-VCH Verlag GmbH & Co. KGaA, Weinheim, Germany, **2000**.
- [53] Y. Sagara, A. Lavrenova, A. Crochet, Y. C. Simon, K. M. Fromm, C. Weder, *Chem. Eur. J.* **2016**, *22*, 4374.
- [54] Y. Sagara, K. Kubo, T. Nakamura, N. Tamaoki, C. Weder, *Chem. Mater.* **2017**, *29*, 1273.
- [55] E. N. Brown, M. R. Kessler, N. R. Sottos, S. R. White, *J. Microencapsulation* **2010**, *20*, 719.
- [56] I. D. Johnston, D. K. McCluskey, C. K. L. Tan, M. C. Tracey, *J. Micromech. Microeng.* **2014**, *24*, 035017.
- [57] M. W. Keller, S. R. White, N. R. Sottos, *Adv. Funct. Mater.* **2007**, *17*, 2399.
- [58] M. W. Keller, N. R. Sottos, *Exp Mech* **2006**, *46*, 725.